Defect Structure around Two Colloids in a Liquid Crystal

O. Guzmán, E. B. Kim, S. Grollau, N. L. Abbott, and J. J. de Pablo*

Department of Chemical Engineering, University of Wisconsin, Madison, Wisconsin 53706-1691, USA

This Letter investigates the defect structures that arise between two colloidal spheres immersed in a nematic liquid crystal. Molecular simulations and a dynamic field theory are employed to arrive at molecular-level and mesoscopic descriptions of the systems of interest. At large separations, each sphere is surrounded by a Saturn ring defect. However, at short separations both theory and simulation predict that a third disclination ring appears in between the spheres, in a plane normal to the Saturn rings. This feature gives rise to an effective binding of the particles. The structures predicted by field theory and molecular simulations are consistent with each other.

PACS numbers: 61.30.Hn, 61.30.Jf

Nematic liquid crystals are characterized by the occurence of disclination lines, topological defects where the average molecular orientation changes abruptly [1]. Recent experiments have shown that topological defects can be exploited in biomolecular sensors [2]. The principle of detection is simple: the presence of biomolecules in an otherwise defect-free nematic perturbs the local ordering of the liquid crystal, triggering the formation of topological defects. Nematics exhibit long-range orientational order, and disclination lines may extend over long distances. The resulting optical signature can be detected with a microscope and crossed polarizers. The amplification factor for this form of detection is remarkable: ten thousand fold, from the scale of a protein (10 nm) to the size of macroscopic disclination lines (0.1 mm).

The design and optimization of liquid crystal based biosensors requires a fundamental understanding of the structure and dynamics of topological defects in the presence of nanometer-scale particles. At the experimental level, Poulin and Weitz have analyzed some of the structures formed when micrometer-sized particles are suspended in a nematic solvent [3], while Lin and co-workers have used optical tweezers to measure the effective interaction potential between two colloidal spheres immersed in a suspension of fd-virus rods [4].

Molecular simulations provide a useful complement to experiments, and have been used to explain the connection between the microscopic and mesoscopic scales. Gay-Berne models, among others, have been useful in studies that relate elastic properties to pair correlation functions [5], analyze defect structures and anchoring orientations around spherical and elongated particles [6], or investigate the phase-ordering dynamics of LC systems [7].

At the mesoscale level, the theoretical description of liquid crystals has been systematically improved from the classical Leslie-Ericksen and Doi theories [8] to a dynamic field theory of the tensor order parameter [9,10]. Classical theories address either the long-range or short-range order elastic effects that govern LC dynamics. The tensor order parameter formulation includes both effects and can easily incorporate viscous flow. It has been successfully applied to the study of defect structures around pairs of particles in bulk isotropic [11] and confined nematic liquid crystals [12,13]. However, in contrast to literature studies that have relied on a linearized form of the governing equations (e.g., studies of long-range interactions in two or three dimensions [11,14,15]), we solve the full, nonlinear problem, thereby allowing us to also explore short-range interactions and defect structures.

This Letter introduces a new defect structure that is expected to arise around a pair of spherical particles; it consists of three disclination rings, instead of the usual two. It was identified by a dual-pronged approach, combining dynamic field theory and Monte Carlo simulations. To the authors' knowledge, it has not been reported before. We begin by providing the essentials of the simulation and theoretical approaches. (For a complete description of the methods readers are referred to previous publications [13,16].) Next we present and discuss the new defect structure in terms of the order parameter, the director, and the size of the rings as a function of the separation of the spheres. We compare our results to those reported recently for a system of two spheres immersed in the isotropic phase [11]. Finally, some suggestions are offered regarding experiments to detect this new structure and our conclusions are presented.

We begin by considering a system of two spherical particles of radius R suspended in a nematic liquid crystal. Figure 1 illustrates the system with a snapshot from one of our Monte Carlo simulations. The LC is confined by horizontal walls separated by a distance Z_{wall}, while the centers of the spheres are confined to the plane $z = Z_{wall}/2$. The spheres' and walls' surfaces impose homeotropic (i.e., perpendicular) anchoring conditions to the liquid crystal molecules. The vector $\mathbf{r}_{12}$ joins the centers of the spheres.

In the simulations, the LC molecules are represented by a large number (tens of thousands) of soft repulsive Gay-Berne ellipsoids. Advanced Monte Carlo methods are required to overcome the free energy barriers that prevent
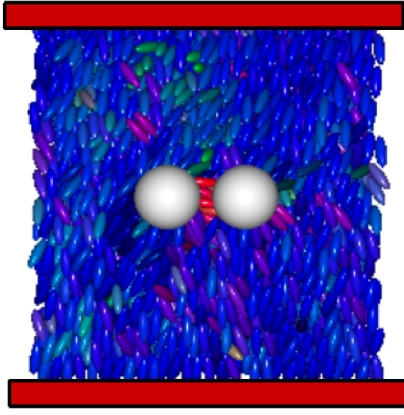
FIG. 1 (color online). Two spheres dispersed in a liquid crystal, with homeotropic (perpendicular) anchoring at the spheres' surface and the confining walls. Periodic boundary conditions are applied in the x and y directions. Colors (online only) indicate orientations, from vertical (blue) to horizontal (red). This snapshot from one of our simulations shows a layer of molecules anchored at both spheres.

appropriate sampling with ordinary schemes. Conventional techniques (e.g., multicanonical ensembles, umbrella sampling) are not easily applicable because they require accurate initial guesses for the shape and position of these barriers. However, an expanded ensemble–density of states method (EXEDOS) has been recently developed to estimate the barriers on the fly [16]. With the EXEDOS method, the LC configurations are sampled uniformly for all separations r_{12}, and the simulations therefore provide reliable information about the interaction energies and associated defect structures.

The orientational structures in the system can be analyzed in terms of the tensor order parameter $\mathbf{Q}$ [9]. This tensor is the result of a coarse-graining procedure, from detailed molecular information to a mesoscopic field that depends on position and time. To define $\mathbf{Q}$, consider a small volume V around a given point $\mathbf{r}$ in the system, and the molecules $\alpha = 1, ..., N$ that are present in it at time t. The Gay-Berne molecules can be pictured as elongated ellipsoids. The lengths of the long and short axes of the molecules are σ_1 and σ_0, respectively. (In this work, $\sigma_1/\sigma_0 = 3$.) The orientation of each ellipsoid is defined by the unit vector $\mathbf{u}^\alpha$ in the direction of its long axis. The Cartesian components of $\mathbf{Q}$ are given by [1]

$$Q_{ij} = \frac{1}{N}\int_V \sum_\alpha \left(u_i^\alpha u_j^\alpha - \frac{1}{3}\delta_{ij}\right)\delta(\mathbf{r} - \mathbf{r}^\alpha)d\mathbf{r}. \qquad (1)$$

The scalar order parameter S (also denoted by P_2) is proportional to the largest eigenvalue λ_{max} of $\mathbf{Q}$, $S = 3\lambda_{max}/2$, while the director $\mathbf{n}$ is the unit-length eigenvector associated with λ_{max}.

In the dynamic field theory considered here, the free energy density is expressed in terms of $\mathbf{Q}$ and its derivatives [17]. The short-range order contribution is represented by a Landau–de Gennes power series expansion,

$$\mathcal{F}_s = \int \frac{A}{2}\left(1 - \frac{U}{3}\right)\mathrm{tr}(\mathbf{Q}^2) - \frac{AU}{3}\mathrm{tr}(\mathbf{Q}^3) + \frac{AU}{4}\mathrm{tr}(\mathbf{Q}^2)^2 d\mathbf{r}. \qquad (2)$$

The long-range elasticity contribution is given in terms of gradients of the components of $\mathbf{Q}$; in the one-elastic constant approximation this elastic free energy reduces to

$$\mathcal{F}_e = \int \frac{L_1}{2}(\partial_k Q_{ij})(\partial_k Q_{ij})d\mathbf{r}. \qquad (3)$$

The total free energy of the system is $\mathcal{F} = \mathcal{F}_s + \mathcal{F}_e$ [18].

The coefficients A, U, and L_1 in Eqs. (2) and (3) are phenomenological parameters that depend on the liquid crystal of interest. Nevertheless, they can be assigned a microscopic interpretation [9]: the coefficient A corresponds to Nk_BT/V, while U is proportional to $\sigma_1\sigma_0^2 N/V$. Equation (2) describes the excluded volume effects that drive the isotropic-nematic (I-N) phase transition. In this model, the I-N transition occurs at $U = 2.7$. The coefficient L_1 in Eq. (3) is a material-specific elastic constant.

The evolution of $\mathbf{Q}$ is determined by the functional derivative of the system's free energy with respect to the tensor order parameter [9,19]:

$$\frac{\partial \mathbf{Q}}{\partial t} = \Gamma\left(-\frac{\delta\mathcal{F}}{\delta\mathbf{Q}} + \frac{\delta_{ij}}{3}\mathrm{tr}\left(\frac{\delta\mathcal{F}}{\delta\mathbf{Q}}\right)\right). \qquad (4)$$

Here, $\Gamma = 6D^*/[1 - 3\,\mathrm{tr}(\mathbf{Q}^2)/2]$ and D^* is the rotational diffusivity coefficient for the molecules forming the LC. We solve the evolution equation (4) numerically by a finite difference method. The calculations are performed with a set of parameters A, U, L_1, and D^* representative of a low-molecular-weight liquid crystal (e.g., pentylcyanobiphenyl, 5CB) [1,20], which has been used in previous theoretical studies [13,21]: $A = 1$, $L_1 = 0.55$, $D^* = 0.35$ [22]. For the isotropic and nematic phases, we used $U = 1$ and $U = 4.8$, respectively. The bare coherence length for the fluid [13], $\xi = (18L_1/AU)^{1/2}$, is $\xi = 1.46R$ for the isotropic phase and $\xi = 0.67R$ for the nematic phase.

As an initial condition, we used a uniaxial field $Q_{ij} = S^0(n_i^0 n_j^0 - \delta_{ij}/3)$, where S^0 is the equilibrium value of S in the bulk nematic. We started from either a totally uniform or a totally random tensor field by choosing $\mathbf{n}^0$ as (i) a constant, given by the unit normal to the walls, or (ii) a random vector on the unit sphere. The same defect configurations were obtained in both cases.

If we examine the system at various separations between the spheres' surfaces, $s = r_{12} - 2R$, we observe that, consistent with previous reports [23], for large s each particle is surrounded by a Saturn ring disclination line. However, for $s < R$ we observe a new structure (see Fig. 2): two incomplete Saturn rings connected to a third ring normal to $\mathbf{r}_{12}$.

In Fig. 3, we compare the structure of the three-ring defect obtained from theory and simulation for $s/R = 0.3$ with $R = 3\sigma_0$. In both cases, the director field is shown
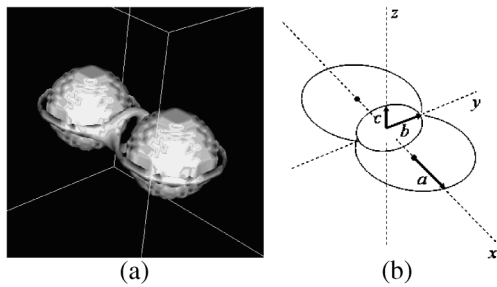
FIG. 2. New three-ring disclination structure around two spheres at a separation $s/R = 0.3$: (a) Contour plot $S = 0.26$; (b) Size of the rings: a (radius of the Saturn rings), b (radius of the third ring along the y axis), and c (radius of the third ring along the z axis).

superimposed on a contour plot of the scalar order parameter. Both theory and simulation display the third ring in addition to the usual Saturn rings. In these plots we can observe how the strength of the scalar order parameter decreases continuously from its bulk value to a minimum at the disclinations. In contrast to field theory, the Monte Carlo results show layers of low and high values of S close to the spheres' surface. The origin of these S layers can be traced to the layering of the LC molecules in the vicinity of the spheres' surface, as reported in a previous publication for different systems [13].

The presence of the third disclination line can be understood by the following argument. In the vicinity of the outer hemispheres (those facing away from each other) the bulk director is in conflict with the local homeotropic anchoring, therefore a Saturn ring disclination is formed. In contrast, when the spheres are close to each other, the local ordering can persist between the inner hemispheres and one can see a "bridge" of director field lines joining the spheres (see Fig. 3). At the microscopic level, one can observe in Fig. 1 a layer of Gay-Berne molecules bridging the inner hemispheres. The third ring disclination line lies at the border of the bridging layer, where molecules abruptly align with the bulk director instead of the line connecting the sphere centers.

In this system, the boundary conditions at the walls single out the z direction, thus the symmetry between the

y and z directions is broken. This asymmetry allows for the possibility that the third ring is not circular. To find out if this is the case, three radii are introduced [see Fig. 2(b)]: a, the radius of the Saturn rings; b, the radius of the third ring along the y axis; and c, the radius of the third ring along the z axis. Plotting the ratios a/R, b/R, and c/R as functions of the separation s/R, as in Fig. 4, we observe that $a > b \geq c$. We also observe that the Saturn rings' size remains constant as the third ring shrinks monotonically when the spheres move away from each other.

Galatola et al. have analyzed a related system using field theory: two spheres immersed in the isotropic phase at the onset of the isotropic-nematic transition [11]. They predicted a single-ring structure, also in the plane normal to $\mathbf{r}_{12}$. We have reproduced this structure with our field theory and Monte Carlo simulations. In contrast to the nematic system, however, the size of the single ring in the isotropic phase increases with the spheres' separation; this means that it is easier to expand the ring in the isotropic case. A way to understand this is to consider the line tension of the rings, i.e., their average free energy per unit length. In the isotropic case, the ring lies at the border of the region where S becomes uniformly zero. Therefore, the ring's free energy density contribution will be small, and so will the line tension be.

What type of experiments would be able to detect this novel structure? First, we must point out that this structure is not expected to arise for large particles in the bulk [3]. The reason is that for these large particles Saturn rings are not stable. Instead, the stable structures are hyperbolic point defects, also known as hedgehogs [1]. For small particles of tens of micrometers in diameter, however, Saturn rings can be stabilized by confinement (note that this is a question that remains open) [23,24]. In this case, it would not be advantageous to look for the three-ring defects in randomly quenched systems with many particles. In such systems the bulk director $\mathbf{n}$ and the separation vector $\mathbf{r}_{12}$ would rarely be orthogonal, and the separation between particles would be difficult to control.

A promising alternative would be to use optical tweezers to bring two particles close to each other in a liquid
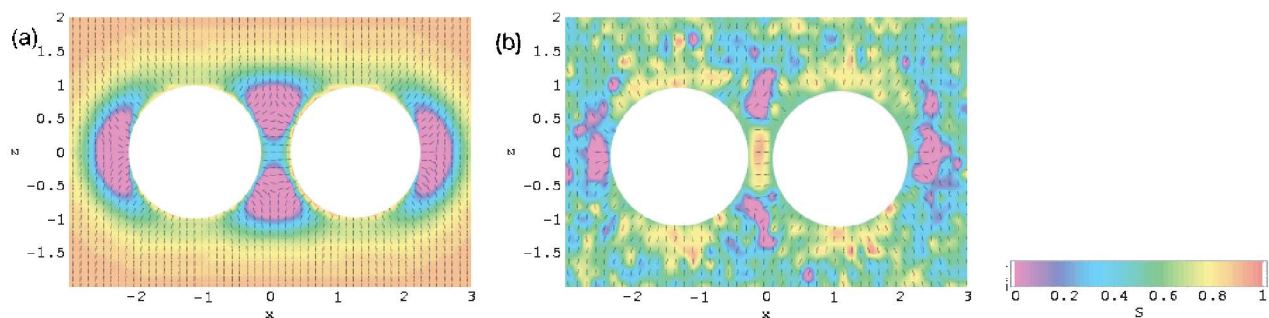

FIG. 3 (color online).   Director and scalar order parameter maps obtained from (a) field theory and (b) Monte Carlo simulations.
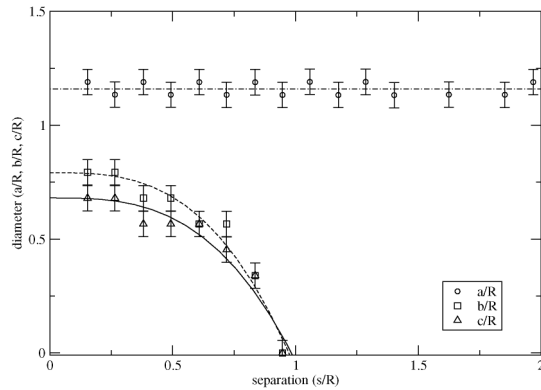
FIG. 4. Ring radii obtained from field theory calculations as a function of the sphere separation. The lines are guides to the eye.

crystal host confined between two plates [4]. An advantage offered by this method is the control over the spheres' position and orientation with respect to a well-defined bulk director. Operating the tweezers in a birefringent material and minimizing the effect of the strong electromagentic fields of the lasers on the structure of the LC are challenges to overcome. A different method, based on the magnetic manipulation of spherical droplets filled with ferrofluid, could also be useful to prepare the required particle configurations and even measuring attractive forces between them [25].

In conclusion, this Letter shows the need to account for the reorganization of defects in situations where linear superposition approximations do not apply. Using molecular simulations and a full tensor formalism, we have uncovered a new defect structure around a pair of nanoscopic particles immersed in a nematic liquid crystal: two incomplete Saturn rings and a third ring, normal to the line connecting the centers of mass of the spheres. The third ring shrinks monotonically as the interparticle distance increases, until it vanishes. The dynamic field theory is able to reproduce the results of simulations down to scales comparable to the molecular length, thereby indicating that the theory is capable of describing both mesoscale and molecular-level phenomena.

*Electronic address: depablo@engr.wisc.edu

[1] P. G. de Gennes and J. Prost, *The Physics of Liquid Crystals* (Clarendon Press, Oxford, 1993); P. M. Chaikin and T. C. Lubensky, *Principles of Condensed Matter Physics* (Cambridge University Press, Cambridge, 1995).

[2] J. A. van Nelson, S. R. Kim, and N. L. Abbott, Langmuir **18**, 5031 (2002); Y. Y. Luk, M. L. Tingey, D. J. Hall, B. A. Israel, C. J. Murphy, P. J. Bertics, and N. L. Abbott, Langmuir **19**, 1671 (2003).

[3] P. Poulin and D. A. Weitz, Phys. Rev. E **57**, 626 (1998).

[4] K.-H. Lin, J. C. Crocker, A. C. Zeri, and A. G. Yodh, Phys. Rev. Lett. **87**, 088301 (2001).

[5] J. Stelzer, L. Longa, and H.-R. Trebin, J. Chem. Phys. **103**, 3098 (1995).

[6] D. Andrienko, G. Germano, and M. P. Allen, Phys. Rev. E **63**, 041701 (2001); D. Andrienko and M. P. Allen, Phys. Rev. E **65**, 021704 (2002); D. Andrienko and M. P. Allen, G. Skacej, and S. Zumer, Phys. Rev. E **65**, 041702 (2002).

[7] J. L. Billeter, A. M. Smondyrev, G. B. Loriot, and R. A. Pelcovits, Phys. Rev. E **60**, 6831 (1999).

[8] F. M. Leslie, in *Theory of Flow Phenomena in Liquid Crystals: Advances in Liquid Crystals*, edited by G. Brown (Academic Press, New York, 1979), Vol. 4, pp. 1–81; M. Doi and S. F. Edwards, *The Theory of Polymer Dynamics* (Clarendon Press, Oxford, 1986).

[9] A. N. Beris and B. J. Edwards, *Thermodynamics of Flowing Systems* (Oxford University Press, New York, 1994).

[10] A. D. Rey and T. Tsuji, Macromol. Theory Simul. **7**, 623 (1998).

[11] P. Galatola and J.-B. Fournier, Phys. Rev. Lett. **86**, 3915 (2001); P. Galatola, J.-B. Fournier, and H. Stark, Phys. Rev. E **67**, 031404 (2003).

[12] H. Stark, J. Stelzer, and R. Bernhard, Eur. Phys. J. B **10**, 515 (1999).

[13] S. Grollau, E. B. Kim, O. Guzman, N. L. Abbott, and J. J. de Pablo, J. Chem. Phys. **119**, 2444 (2003).

[14] M. Tasinkevych, N. M. Silvestre, P. Patricio, and M. M. Telo Da Gama, Eur. Phys. J. E **9**, 341 (2002).

[15] R. W. Ruhwandl and E. M. Terentjev, Phys. Rev. E **55**, 2958 (1997).

[16] E. Kim, R. Faller, Q. Yan, N. L. Abbott, and J. J. de Pablo, J. Chem. Phys. **117**, 7781 (2002); F. Calvo, Mol. Phys. **100**, 3421 (2002).

[17] We are concerned with the equilibrium behavior in the absence of an imposed flow, and it is therefore admissible to look for long-time solutions neglecting viscous flow.

[18] In the molecular simulations, we observe strong anchoring at all interfaces: $\mathbf{Q}$ is locked to its preferred homeotropic value. As a first approximation, we do not include a surface free energy term in $\mathcal{F}$.

[19] In Eq. (4), it is assumed that the functional derivative has been symmetrized: $[\delta \mathcal{F}/\delta \mathbf{Q}]_{ij} \equiv \frac{1}{2}[(\delta \mathcal{F}/\delta Q_{ij}) + (\delta \mathcal{F}/\delta Q_{ji})]$. For our model's $\mathcal{F}$, both terms are identical.

[20] J. Stelzer and R. Bernhard, cond-mat 0012394.

[21] G. Toth, C. Denniston, and J. M. Yeomans, Phys. Rev. Lett. **88**, 105504 (2002); G. Toth, C. Denniston, and J. M. Yeomans, Phys. Rev. E **67**, 051705 (2003).

[22] These values correspond to $L_1 = 8.73$ pN, $D^* = 3.50$ Pa^{-1} s^{-1} and are comparable with those in [20,21].

[23] S. Grollau, N. L. Abbott, and J. J. de Pablo, Phys. Rev. E **67**, 011702 (2003).

[24] Y. Gu and N. L. Abbott, Phys. Rev. Lett. **85**, 4719 (2000).

[25] P. Poulin, V. Cabuil, and D. A. Weitz, Phys. Rev. Lett. **79**, 4862 (1997).